European Journal of Chemistry 5 (1) (2014) 6-10

European Journal of Chemistry
Journal homepage: www.eurjchem.com

Crystal structures of racemic and enantiomeric 5-isopropyl-5-methylhydantoin

Masaki Ichitani, Soh-ichi Kitoh, Keiko Tanaka, Shuhei Fujinami, Mitsuhiro Suda, Mitsunori Honda and Ko-Ki Kunimoto *

Graduate School of Natural Science and Technology, Kanazawa University, Kakuma-machi, Kanazawa 920-1192, Japan

**Corresponding author at: Graduate School of Natural Science and Technology, Kanazawa University, Kakuma-machi, Kanazawa 920-1192, Japan. Tel.: +81.76.2646292. Fax: +81.76.2646292. E-mail address: kunimoto@se.kanazawa-u.ac.jp (K.-K. Kunimoto).*

ARTICLE INFORMATION

DOI: 10.5155/eurjchem.5.1.6-10.933

Received: 25 September 2013
Accepted: 06 October 2013
Online: 31 March 2014

KEYWORDS

Hydantoin
Enantiomer
Conglomerate
Crystal structure
Racemic compound
Imidazolidine-2,4-dione

ABSTRACT

Crystal structures of racemic and enantiomeric 5-isopropyl-5-methylhydantoin (IPrMH) have been determined by single crystal X-ray diffraction. Melting temperatures and solid state infrared spectra are also measured. Racemic IPrMH has a lower melting temperature than the pure enantiomer by 25 °C. The infrared spectrum of racemic IPrMH is identical with that of the pure enantiomer. Nevertheless, the racemic IPrMH doesn't crystallize as a conglomerate but as a racemic compound. The racemic and the enantiomeric crystals are very similar to each other in molecular geometries and intermolecular interactions. In the both cases, the molecules are connected *via* N–H···O hydrogen bonds to form $R^2_2(8)$ rings, and these rings are linked into infinite one-dimensional tapes. In the racemic crystal, a single tape is composed of single enantiomer and itself is homochiral.

1. Introduction

Hydantoins (imidazolidine-2,4-diones) and 2-thiohydantoins (2-thioxoimidazolidin-4-ones) are two classes of 5-membered heterocycles containing two nitrogens in an ureide and a thioureide configuration, respectively. Due to their diverse biological and pharmacological properties, these compounds have been used in a wide variety of applications [1]. For instance, hydantoins have been widely used as antiarrhythmic and antihypertensive [2,3], antiviral [4], antineoplastic [5], antitumoral [6] and anticonvulsant agents [7,8]. Thiohydantoins are known for their uses as hypolipidemic [9], antimutagenic [10] and anticarcinogenic agents [11]. In addition, both compounds are used as herbicides [12] and fungicides agents [13].

These classes of compounds commonly carry the amide and/or the thioamide groups in a molecule, which provides equal number of hydrogen-bond proton donor (D) and acceptor (A) in the D-A-D-A sequence. This unique structural feature endows the compounds with unique physicochemical and biological properties [14,15]. We have studied the crystal structures of a series of hydantoins and 2-thiohydantoins in order to get information on the factors controlling the molecular environment in the crystal [16-22].

For a chiral compound, the racemic compound and the enantiomer essentially possess different crystal structures. These differences in crystal structures lead to the different physicochemical properties of the racemic and the enantiomeric compounds. Thus, comparison of the racemic and the enantiomeric crystal structures offers a unique opportunity to study the differences in the intermolecular interactions and the molecular packings involving the same molecule in different crystalline environments.

In this study, the racemate and (*S*)-enantiomer of 5-isopropyl-5-methylhydantoin ((*rac*)-IPrMH) and (*S*)-IPrMH) have been synthesized (Figure 1). These crystal structures are analyzed by the single crystal X-ray diffraction. Melting temperatures and solid state infrared (IR) spectra of both crystals are also discussed.

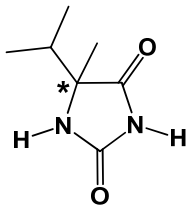

Figure 1. Chemical structure of 5-isopropyl-5-methylhydantoin (IPrMH).

2. Experimental

2.1. Instrumentation

Table 1. Crystal data and structure refinement.

	(*rac*)-IPrMH	(*S*)-IPrMH
Empirical formula	$C_7H_{12}N_2O_2$	$C_7H_{12}N_2O_2$
Formula weight	156.19	156.19
Temperature	123(2) K	123(2) K
Wavelength	0.71070 Å	0.71070 Å
Crystal system	Monoclinic	Monoclinic
Space group	$P2_1/n$	$P2_1$
Unit cell dimensions	a = 11.0943(18) Å	a = 6.8048(12) Å
	b = 7.1033(11) Å	b = 7.0202(12) Å
	c = 11.0940(18) Å	c = 8.8865(16) Å
	β = 105.636(3) °	β = 90.015(4) °
Volume	841.9(2) Å^3	424.52(13) Å^3
Z	4	2
Density (calcd.)	1.232 g/cm^3	1.222 g/cm^3
Absorption coefficient	0.091 mm^{-1}	0.091 mm^{-1}
F(000)	336	168
Crystal size/color	0.35 × 0.15 × 0.08 mm^3/colorless	0.35 × 0.15 × 0.05 mm^3/colorless
Theta range for data collection	3.04 to 27.48 °	4.76 to 27.42 °
Index ranges	$-14 \le h \le 14$	$-8 \le h \le 8$
	$-9 \le k \le 9$	$-9 \le k \le 8$
	$-12 \le l \le 14$	$-11 \le l \le 11$
Reflections collected	8776	4583
Independent reflections	1908 [$R_{(int)}$ = 0.0219]	1028 [$R_{(int)}$ = 0.0225]
Completeness	99.0 %	98.0 %
Absorption correction	Multi-scan [24]	Multi-scan [24]
Max. and min. transmission	0.9927 and 0.9687	0.9955 and 0.9690
Refinement method	Full-matrix least-squares on F^2	Full-matrix least-squares on F^2
Data/restraints/parameters	1908/0/111	1028/1/111
Goodness-of-fit on F^2	1.041	1.092
Final R indices [I > 2sigma(I)]	R_1 = 0.0437, wR_2 = 0.1174	R_1 = 0.0299, wR_2 = 0.0789
R indices (all data)	R_1 = 0.0478, wR_2 = 0.1207	R_1 = 0.0316, wR_2 = 0.0800
Largest diff. peak and hole	0.341 and −0.191 e Å^{-3}	0.238 and −0.117 e Å^{-3}
Measurement	Rigaku/MSC Mercury CCD diffractometer	Rigaku/MSC Mercury CCD diffractometer
Program system	*Crystal Structure* [27]	*Crystal Structure* [27]
Structure determination	Direct methods (*SIR2008* [25])	Direct methods (*SIR2008* [25])
CCDC no	962338	962341

The melting points were measured using a Shimadzu DSC-60 differential scanning calorimeter (DSC) equipment. The infrared (IR) spectra were recorded on a Horiba FT-720 Fourier transform infrared spectrometer. IR measurements were carried out by the KBr method at 64 scans per spectrum with 4 cm^{-1} resolution. ^{1}H NMR spectra (500 MHz) and ^{13}C NMR spectra (125 MHz) were recorded on a JEOL JNM-ECA 500 spectrometer.

The X-ray diffraction data were collected at 123(2) K by ω scan technique on a Rigaku/MSC Mercury CCD diffractometer [23] equipped with graphite-monochromatized MoK_α radiation (λ = 0.71070 Å). The data were corrected for Lorentz-polarization and absorption effects [24]. These structures were solved by direct methods using SIR2008 program [25] and refined by a full-matrix least-squares calculation on F^2 using SHELXL-97 [26]. All calculations were performed using Crystal Structure software package [27].

The absolute configuration of (*S*)-IPrMH has not been established by anomalous dispersion effects in diffraction measurements on the crystal. The enantiomer has been assigned by reference to an unchanging chiral centre in the synthetic procedure [28]. Non-hydrogen atoms were refined anisotropically. The hydrogen atoms bonded to nitrogen atoms were located in a difference map and refined freely. The remaining hydrogen atoms were positioned geometrically (C–H = 0.98 or 1.00 Å) and refined using a riding model, with U_{iso}(H) = 1.2 U_{eq}(C). Structures were visualized using ORTEP-3 for windows [29] and Mercury [30]. Details on data collection and refinement are given in Table 1.

2.2. Synthesis

(*rac*)-5-Isopropyl-5-methylhydantoin was synthesized by slight modification of a literature method [28]. A 1:3 mixture of α-methyl-*DL*-valine (0.20 g, 1.53 mmol) and urea (0.27 g, 4.57 mmol) were allowed to react directly in the absence of solvent at 150 °C for 2 h. This reaction was carried out in a 30 mL round-bottom flask under stirring using an oil bath as the heat source. After the reaction was complete, water was added while the flask was still warm. The solution was reheated to dissolve all the solids and allowed to cool to room temperature, then placed in a refrigerator for 3 h. The colorless crystals removed by vacuum filtration were further purified by flash column chromatography using hexane and ethyl acetate as eluents. Single crystals suitable for X-ray diffraction were obtained by recrystallization from an aqueous solution.

(*S*)-5-Isopropyl-5-methylhydantoin was prepared through the reaction of α-methyl-*L*-valine (0.20 g, 1.53 mmol, Bachem AG, Bubendorf, Switzerland) and urea (0.27 g, 4.57 mmol) by the same procedure. Single crystals suitable for X-ray diffraction were obtained by recrystallization from an aqueous solution.

(rac)-5-Isopropyl-5-methylhydantoin ((*rac*)-IPrMH): Color: Colorless. Yield: 50%. M.p.: 171 °C. FT-IR (KBr, ν, cm^{-1}): 3218 ν(NH), 1765 ν(C=O), 1720 ν(C=O), 1434 ν(CN)+δ(NH). ^{1}H NMR (500 MHz, Aceton-d_6, δ, ppm): 0.90 (d, 3H, J = 6.9 Hz, (CH_3)$_2$-CH), 0.99 (d, 3H, J = 6.9 Hz, (CH_3)$_2$-CH), 1.38 (s, 3H, CH_3-C), 1.97 (sep, 1H, J = 6.9 Hz, (CH$_3$)$_2$-CH), 7.12 (br. s, 1H, NH-CO-NH-CO), 9.58 (br. s, 1H, NH-CO-NH-CO). ^{13}C NMR (125 MHz, Aceton-d_6, δ, ppm): 178.81 (1C, NH-CO-NH-*C*O), 157.60 (1C, NH-*C*O-NH-CO), 66.53 (1C, CH$_3$-*C*), 34.95 (1C, (CH$_3$)$_2$-*C*H), 22.15 (1C, *C*H$_3$-C), 17.23 (1C, (*C*H$_3$)$_2$-CH), 16.44 (1C, (*C*H$_3$)$_2$-CH).

(S)-5-Isopropyl-5-methylhydantoin ((S)-IPrMH): Color: Colorless. Yield: 60%. M.p.: 196 °C. FT-IR (KBr, ν, cm^{-1}): 3218 ν(NH), 1765 ν(C=O), 1720 ν(C=O), 1434 ν(CN)+δ(NH). ^{1}H NMR (500 MHz, Aceton-d_6, δ, ppm): 0.90 (d, 3H, J = 6.9 Hz, (CH_3)$_2$-CH), 0.99 (d, 3H, J = 6.9 Hz, (CH_3)$_2$-CH), 1.37 (s, 3H, CH_3-C), 1.97 (sep, 1H, J = 6.9 Hz, (CH$_3$)$_2$-CH), 7.07 (br. s, 1H, NH-CO-NH-CO), 9.54 (br. s, 1H, NH-CO-NH-CO). ^{13}C NMR (125 MHz, Aceton-d_6, δ, ppm): 178.80 (1C, NH-CO-NH-*C*O), 157.43 (1C, NH-*C*O-NH-CO), 66.51 (1C, CH$_3$-*C*), 34.97 (1C, (CH$_3$)$_2$-*C*H), 22.19 (1C, *C*H$_3$-C), 17.25 (1C, (*C*H$_3$)$_2$-CH), 16.46 (1C, (*C*H$_3$)$_2$-CH).

3. Results and discussion

(*rac*)-IPrMH and (*S*)-IPrMH were synthesized by one-pot reaction of α-methyl-*DL*-valine and α-methyl-*L*-valine with urea, respectively, in the absence of solvent. (*S*)-IPrMH was obtained in an optical pure form without racemization in the present reaction condition.

Table 2 and Figure 2 summarize the melting points and solid state IR spectra of IPrMH. (*rac*)-IPrMH crystal shows a melting point of 171 °C, while (*S*)-IPrMH melts at 196 °C. Thus, the racemic crystal of IPrMH has a lower melting temperature than the enantiopure crystal by 25 °C. As given in Figure 2, the IR spectrum of (*rac*)-IPrMH is identical with that of the pure enantiomer.

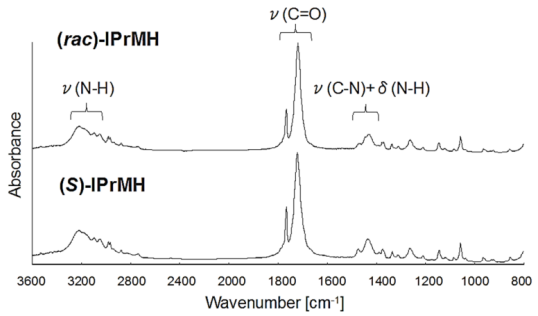

Figure 2. Solid state IR spectra of (*rac*)-IPrMH and (*S*)-IPrMH.

Table 2. Melting points and solid state IR spectra.

	M.p. (°C)	IR (cm^{-1})		
		ν(NH)	ν(C=O)	ν(CN)+δ(NH)
(*rac*)-IPrMH	171	3218	1765, 1720	1434
(*S*)-IPrMH	196	3218	1765, 1720	1434

When a racemate crystallizes as a conglomerate (equimolar mechanical mixtures of two crystalline enantiomers), the melting point of the conglomerate is always lower than that of the pure enantiomer, and the solid state IR spectra of the conglomerate are identical with those of the pure enantiomer [31]. On the other hand, the melting point of a racemic compound (equimolar enantiomers are present in the crystal lattice) is generally higher than that of the pure enantiomer, and the solid state IR spectra of the racemic compound are not identical with those of the pure enantiomer [32].

In the present case, the melting point values and the IR spectra suggest the conglomerate formation for the racemic IPrMH crystals. However, the single crystal X-ray diffraction data has shown that the racemic IPrMH doesn't crystallize as a conglomerate but as a racemic compound. Thus, this study presents the rare case of lower melting racemic and higher melting enantiomeric crystals.

Table 1 shows the crystallographic data. Figure 3 and 4 show the molecular structure and atom-labeling scheme of (*rac*)-IPrMH and (*S*)-IPrMH, respectively. Table 3 summarizes the selected geometric parameters. Figure 5, 6 and 7, 8 show the crystal packing of (*rac*)-IPrMH and (*S*)-IPrMH, respectively. Table 4 shows the hydrogen-bond geometry. As given in Table 1, (*rac*)-IPrMH crystallizes in the monoclinic system with space group $P2_1/n$ and four molecules in a unit cell. (*S*)-IPrMH crystallizes in the monoclinic system with space group $P2_1$ and two molecules in a unit cell.

As given in Figure 3, 4 and Table 3, (*rac*)-IPrMH and (*S*)-IPrMH are very similar in molecular geometries. The hydantoin moieties (N1/C1/O1/N2/C2/O2/C3) for (*rac*)-IPrMH and (*S*)-IPrMH are nearly planar, with maximum deviations of 0.0285(13) Å in N2 and 0.0467(17) Å in N2, respectively. The orientations of the isopropyl groups, defined by the C5, C6 and C7 atoms, relative to these planes are given by the torsion angles N1–C3–C5–C6 of 63.46(14) ° for (*rac*)-IPrMH and 62.8(2) ° for (*S*)-IPrMH. The N1–C1 distances [1.3348(14) Å for (*rac*)-IPrMH; 1.332(2) Å for (*S*)-IPrMH] are shorter than the N2–C1 distances [1.3818(14) Å for (*rac*)-IPrMH; 1.384(2) Å for (*S*)-IPrMH], and the O1–C1–N1 angles [127.31(10) ° for (*rac*)-IPrMH; 127.67(17) ° for (*S*)-IPrMH] are greater than the O1–C1–N2 angles [124.35(10) ° for (*rac*)-IPrMH; 124.06(17) ° for (*S*)-IPrMH].

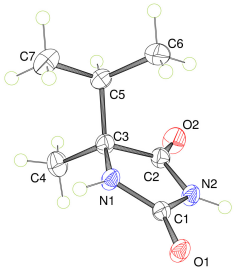

Figure 3. Molecular structure of (*rac*)-IPrMH. Anisotropic displacement ellipsoids are drawn at the 50% probability level.

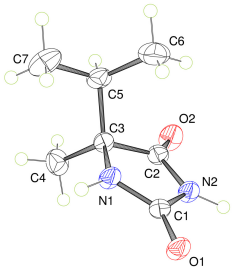

Figure 4. Molecular structure of (*S*)-IPrMH. Anisotropic displacement ellipsoids are drawn at the 50% probability level.

Table 3. Selected geometric parameters (Å, °).

Geometric parameters	(*rac*)-IPrMH	(*S*)-IPrMH
Bond lengths		
O1–C1	1.2379(14)	1.2376(18)
O2–C2	1.2084(15)	1.202(2)
N1–C1	1.3348(14)	1.332(2)
N1–C3	1.4652(14)	1.4638(19)
N2–C1	1.3818(14)	1.384(2)
N2–C2	1.3751(15)	1.381(2)
C2–C3	1.5366(17)	1.536(2)
Bond angles		
C1–N1–C3	112.83(9)	113.03(15)
C1–N2–C2	111.55(10)	111.42(14)
O1–C1–N1	127.31(10)	127.67(17)
O1–C1–N2	124.35(10)	124.06(17)
N1–C1–N2	108.34(10)	108.27(12)
O2–C2–N2	126.21(11)	126.08(16)
O2–C2–C3	127.02(11)	127.32(15)
N2–C2–C3	106.77(9)	106.60(14)
N1–C3–C2	100.44(8)	100.55(13)
Torsion angles		
N1–C3–C5–C6	63.46(14)	62.8(2)
N1–C3–C5–C7	−60.23(13)	−61.22(18)
C2–C3–C5–C6	−47.44(14)	−48.4(2)
C2–C3–C5–C7	−171.14(10)	−172.46(14)
C4–C3–C5–C6	−169.84(12)	−170.46(19)
C4–C3–C5–C7	66.46(13)	65.47(19)

In (*rac*)-IPrMH crystal (Figure 5, 6 and Table 4), the amide N1–H and N2–H of one molecule are hydrogen-bonded to the amide O1=C1 groups of neighboring molecules to form $R^2_2(8)$ [33] rings [N1···O1^{i} 2.8334(13) Å, N1–H···O1^{i} 168.9(14) °; N2···O1^{ii} 2.8226(13) Å, N2–H···O1^{ii} 168.9(16) °; symmetry codes: (*i*) −*x*+1/2, *y*−1/2, −*z*+3/2; (*ii*) −*x*+1/2, *y*+1/2, −*z*+3/2]. The amide O2=C2 groups aren't hydrogen-bonded. These rings are linked into infinite one-dimensional tapes around a two-

fold screw axis along the *b* axis. A single tape is composed of single enantiomer and itself is homochiral.

Table 4. Hydrogen-bond geometry (Å, °) (D-donor; A-acceptor; H-hydrogen).

D–H···A *	D–H	H···A	D···A	D–H···A
(*rac*)-IPrMH				
N1–H···O1^{i}	0.903(17)	1.944(15)	2.8334(13)	168.9(14)
N2–H···O1^{ii}	0.862(17)	1.970(15)	2.8226(13)	168.9(16)
(*S*)-IPrMH				
N1–H···O1^{iii}	0.84(3)	2.02(3)	2.841(2)	166(2)
N2–H···O1^{iv}	0.94(2)	1.89(2)	2.819(2)	169(2)

* Symmetry codes: (*i*) −*x*+1/2, *y*−1/2, −*z*+3/2; (*ii*) −*x*+1/2, *y*+1/2, −*z*+3/2; (*iii*) −*x*, *y*+1/2, −*z*+2; (*iv*) −*x*, *y*−1/2, −*z*+2.

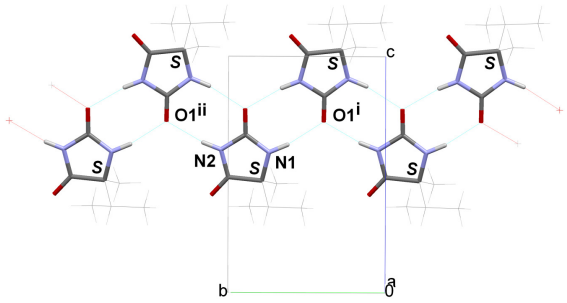

Figure 5. Crystal packing of (*rac*)-IPrMH viewed down the *a* axis, showing the hydrogen-bonded one-dimensional (*S*)-tape running along the *b* axis. Hydrogen bonds are shown as dashed cyan lines (see Table 4 for details).

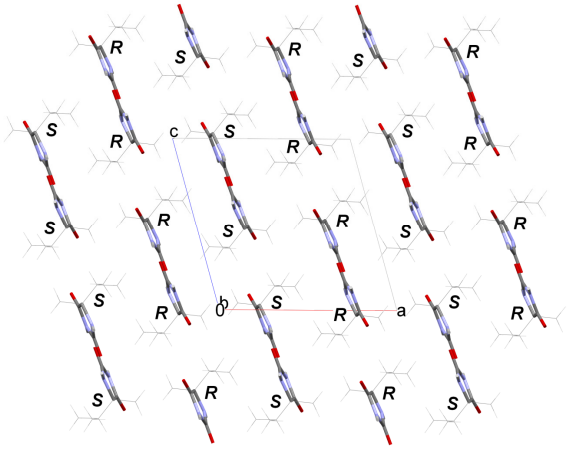

Figure 6. Crystal packing of (*rac*)-IPrMH viewed down the *b* axis, showing the stacking of (*S*)-tapes and (*R*)-tapes.

As shown in Figure 7 and Table 4, (*S*)-IPrMH crystal is very similar to (*rac*)-IPrMH crystal in N–H···O hydrogen-bonding pattern [N1···O1^{iii} 2.841(2) Å, N1-H···O1^{iii} 166(2) °; N2···O1^{iv} 2.819(2) Å, N2–H···O1^{iv} 169(2) °; symmetry codes: (*iii*) −*x*, *y*+1/2, −*z*+2; (*iv*) −*x*, *y*−1/2, −*z*+2]. On the other hand, (*S*)-IPrMH crystal is quite different from (*rac*)-IPrMH crystal in the packing mode of the one-dimentional tapes by the hydrogen bonds. As shown in Figure 6, (*rac*)-IPrMH crystal is formed by the alternate packing of two different kinds of homochiral tapes, represented as (*S*)-tapes and (*R*)-tapes. (*S*)-IPrMH crystal is formed by the packing of only (*S*)-tapes (Figure 8).

4. Conclusion

The racemic IPrMH exhibits lower melting temperature than the pure enantiomer by 25 °C. The solid state IR spectrum of the racemic IPrMH is identical with that of the pure enantiomer. These experimental results suggest the formation of conglomerate crystals. Nevertheless, the racemic IPrMH doesn't crystallize as a conglomerate but as a racemic compound. In the racemic and the enantiomeric crystals, the molecular geometries and the intermolecular interactions are very similar to each other. In the both cases, the amide N1–H and N2–H of one molecule are hydrogen-bonded to the amide O1=C1 groups of neighboring molecules to form $R^2_2(8)$ rings, and these rings are linked into infinite one-dimensional tapes. In the racemic crystal, a single tape is composed of single enantiomer and itself is homochiral.

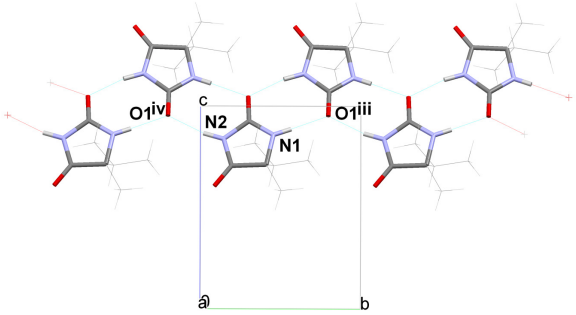

Figure 7. Crystal packing of (*S*)-IPrMH viewed down the *a* axis, showing the hydrogen-bonded one-dimensional tape running along the *b* axis. Hydrogen bonds are shown as dashed cyan lines (see Table 4 for details).

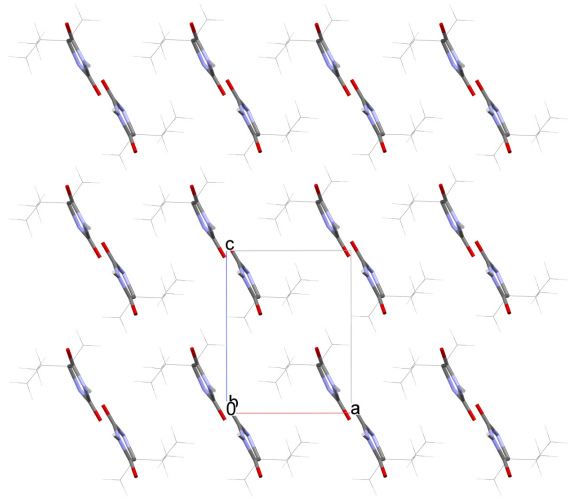

Figure 8. Crystal packing of (*S*)-IPrMH viewed down the *b* axis, showing the stacking of (*S*)-tapes.

Supplementary materials

CCDC-962338 and CCDC-962341 contain the supplementary crystallographic data for this paper. These data can be obtained free of charge *via* www.ccdc.cam.ac.uk/data_request/cif, or by e-mailing data_request@ccdc.cam.ac.uk , or by contacting The Cambridge Crystallographic Data Centre, 12 Union Road, Cambridge CB2 1EZ, UK; fax: +44(0)1223-336033.

References

[1]. Mutschler, E.; Derendorf, H. Drug Actions, Basic Principles and Therapeutic Aspects, Medpharm Scientific Publishers, Stuttgart, 1995.
[2]. Knabe, J.; Baldauf, J.; Ahlhem, A. *Pharmazie* **1997**, *52*, 912-919.
[3]. Dylag, T.; Zygmunt, M.; Maciag, D.; Handzlik, J.; Bednarski, M.; Filipek, B.; Kiec-Kononowicz, K. *Eur. J. Med. Chem.* **2004**, *39*, 1013-1027.
[4]. Opacic, N.; Barbaric, M.; Zorc, B.; Cetina, M.; Nagl, A.; Frkovic, D.; Kralj, M.; Pavelic, K.; Balzarini, J.; Andrei, G.; Snoeck, R.; De Clercq, E.; Raic-Malic, S.; Mintas, M. *J. Med. Chem.* **2005**, *48*, 475-482.
[5]. Lattmann, E.; Ayuko, W. O.; Kinchinaton, D.; Langley, C. A.; Singh, H.; Karimi, L.; Tisdale, M. J. *J. Phar. Pharmacol.* **2003**, *55*, 1259-1265.

[6]. Carmi, C.; Cavazzoni, A.; Zuliani, V.; Lodola, A.; Bordi, F.; Plazzi, P. V.; Alfieri, R. R.; Petronini, P. G.; Mor, M. *Bioorg. Med. Chem. Lett.* **2006**, *16*, 4021-4025.
[7]. Singh, G.; Driever, P. H.; Sander, J. W. *Brain* **2005**, *128*, 7-17.
[8]. Kaindl, A. M.; Asimiadou, S.; Manthey, D.; Hagen, M. V.; Turski, L.; Ikonomidou, C. *Cell. Mol. Life Sci.* **2006**, *63*, 399-413.
[9]. Tompkins, J. E. *J. Med. Chem.* **1986**, *29*, 855-859.
[10]. Takahashi, A.; Matsuoka, H.; Yamada, K.; Uda, Y. *Food Chem. Toxicol.* **2005**, *43*, 521-528.
[11]. Al-Madi, S. H.; Al-Obaid, A. M.; El-Subbagh, H. I. *Anti-Cancer Drugs* **2001**, *12*, 835-839.
[12]. Shiozaki, M. *Carbohyd. Res.* **2002**, *337*, 2077-2088.
[13]. Marton, J.; Enisz, J.; Hosztafi, S.; Timar, T. *J. Agric. Food. Chem.* **1993**, *41*, 148-152.
[14]. Jha, S.; Silversides, J. D.; Boyle, R. W.; Archibald, S. J. *Cryst. Eng. Comm.* **2010**, *12*, 1730-1739.
[15]. Cruz-Cabeza, A. J.; Schwalbe, C. H. *New J. Chem.* **2012**, *36*, 1347-1354.
[16]. Ogawa, T.; Kitoh, S.; Ichitani, M.; Kuwae, A.; Hanai, K.; Kunimoto, K. *Anal. Sci. X-ray Struct. Anal. Online* **2007**, *23*, x199-x200.
[17]. Ogawa, T.; Kitoh, S.; Okagawa, M.; Ichitani, M.; Kuwae, A.; Hanai, K.; Kunimoto, K. *Anal. Sci. X-ray Struct. Anal. Online* **2007**, *23*, x201-x202.
[18]. Kunimoto, K.; Ichitani, M.; Ogawa, T.; Kitoh, S.; Kuwae, A.; Hanai, K. *Spectrosc. Lett.* **2009**, *42*, 73-80.
[19]. Ogawa, T.; Okumura, H.; Honda, M.; Suda, M.; Fujinami, S.; Kuwae, A.; Hanai, K.; Kunimoto, K. *Anal. Sci. X-ray Struct. Anal. Online* **2009**, *25*, 91-92.
[20]. Taniguchi, K.; Okumura, H.; Honda, M.; Suda, M.; Fujinami, S.; Kuwae, A.; Hanai, K.; Maeda, S.; Kunimoto, K. *Anal. Sci. X-ray Struct. Anal. Online* **2009**, *25*, 93-94.
[21]. Ichitani, M.; Kitoh, S.; Fujinami, S.; Suda, M.; Honda, M.; Kunimoto, K. *Acta Cryst. E* **2013**, *69*, o953-o953.
[22]. Ichitani, M.; Kitoh, S.; Tanaka, K.; Fujinami, S.; Suda, M.; Honda, M.; Kuwae, A.; Hanai, K.; Kunimoto, K. *Eur. J. Chem.* **2013**, *4*, 350-352.
[23]. Rigaku *CrystalClear*, Rigaku Corporation, Tokyo, Japan, 2006.
[24]. Rigaku REQAB, Rigaku Corporation, Tokyo, Japan, 1998.
[25]. Burla, M. C.; Caliandro, R.; Camalli, M.; Carrozzini, B.; Cascarano, G. L.; De Caro, L.; Giacovazzo, C.; Polidori, G.; Siliqi, D.; Spagna, R. *J. Appl. Cryst.* **2007**, *40*, 609-613.
[26]. Sheldrick, G. M. *Acta Cryst. A* **2008**, *64*, 112-122.
[27]. Rigaku *CrystalStructure*, Rigaku Corporation, Tokyo, Japan, 2010.
[28]. Wang, Z. D.; Sheikh, S. O.; Zhang, Y. *Molecules* **2006**, *11*, 739-750.
[29]. Farrugia, L. J. *J. Appl. Cryst.* **2012**, *45*, 849-854.
[30]. Macrae, C. F.; Edgington, P. R.; McCabe, P.; Pidcock, E.; Shields, G. P.; Taylor, R.; Towler, M.; van de Streek, J. *J. Appl. Cryst.* **2006**, *39*, 453-457.
[31]. Mitchell, A. G. *J. Pharm. Pharmaceut. Sci.* **1998**, *1*, 8-12.
[32]. Wilhoit, R. C.; Chan, J.; Hall, K. R. *J. Phys. Chem. Ref. Data* **1985**, *14*, 1-175.
[33]. Etter, M. C. *Acc. Chem. Res.* **1990**, *23*, 120-126.